19

Fabrication of ZnO Based Dye Sensitized Solar Cells

A.P. Uthirakumar
Nanoscience Centre for Optoelectronics and Energy Devices, Sona College of Technology, Salem, Tamilnadu, India

1. Introduction

Why solar power is considered as one of the ultimate future energy resources? To answer this, drastic depletion of fossil fuels and the challenges ahead on needs for the specific requirements are the major causes for the need alternative power. At the beginning of February, 2007, the Intergovernmental Panel on Climate Change (*IPCC*) presented a report concluding that global concentrations of carbon dioxide, methane and nitrous oxide have increased markedly as a result of human activities since 1750. The report states that the increase in carbon dioxide, the most important greenhouse gas, is primarily due to fossil fuel use. The report further indicates that the increased concentrations of carbon dioxide, methane, and nitrous oxide have increased the average global temperature, a phenomenon known as "global warming". Eventually, if the temperature continues to increase, this will influence our everyday lives, since it changes the conditions of, for example, agriculture and fishing. In order to preserve the surplus energy coming out from the Sun, an alternative technique is necessary for our future energy needs. The potential of using the sun as a primary energy source is enormous. For example, sunlight strikes the Earth in one hour (4.3 × 1020 J) is sufficient to satisfy the more than the globel energy consumed on the planet in a year (4.1 × 1020 J). In other words, it has been calculated that covering 0.1% of the earth's surface area with solar cells of 10% efficiency, corresponding to 1% of desert areas or 20% of the area of buildings and roads, would provide for global electricity consumption. As for as to convert the solar power into the basic electricity, there may be the new technology to be implimented to harvest the solar energy in an effective manner. In this regard, one way to consume solar power, the photovoltaic cell will be suitable one to convert sunlight into electrical energy. The challenge in converting sunlight into electricity via photovoltaic solar cells is dramatically reducing the cost/watt of delivered solar electricity, by approximately a factor of 5–10 times to compete with fossil and nuclear electricity and by a factor of 25–50 to compete with primary fossil energy.

Recently, many of research groups are actively involving to harvest maximum conversion of solar power into electricity. Hence, varieties of new materials that are capable to absorb solar spectrum are successfully prepared in different methods. These new materials should satisfy the following important points to be act as the effective light harvesting materials. It should be efficiently absorb sunlight, should cover the full spectrum of wavelengths in solar radiation, and new approaches based on nanostructured architectures can revolutionize the technology used to produce energy from the solar radiation. The technological development in novel approaches exploiting thin films, organic semiconductors, dye sensitization, and

quantum dots offer fascinating new opportunities for cheaper, more efficient, longer-lasting systems. The conversion from solar energy to electricity is fulfilled by solar-cell devices based on the photovoltaic effect. Many photovoltaic devices have already been developed over the past five decades (Liu et al., 2008). However, wide-spread use is still limited by two significant challenges, namely conversion efficiency and cost (Bagnall et al., 2008). One of the traditional photovoltaic devices is the single-crystalline silicon solar cell, which was invented more than 50 years ago and currently makes up 94% of the market (Chapin et al., 1954). In addition to this other compound semiconductors, such as gallium arsenide (GaAs), cadmium telluride (CdTe), and copper indium gallium selenide, receive much attention because they present direct energy gaps, can be doped to either p-type or n-type, have band gaps matching the solar spectrum, and have high optical absorbance (Afzaal & O'Brien, 2006). These devices have demonstrated single-junction conversion efficiencies of 16–32% (Birkmire, 2001). Although those photovoltaic devices built on silicon or compound semiconductors have been achieving high efficiency for practical use, they still require major breakthroughs to meet the long-term goal of very-low cost.

In case of lowering the cost of production, dye-sensitized solar cells (DSSCs) based on oxide semiconductors and organic dyes or metallorganic-complex dyes have recently emerged as promising approach to efficient solar-energy conversion. The DSSCs are a photoelectrochemical system, which incorporate a porous-structured oxide film with adsorbed dye molecules as the photosensitized anode. A typical DSSC system composed of a mesoporous titanium dioxide (TiO_2) film on a transparent conductor. Dye molecules are absorbed on the entire porous TiO_2 that is perfused with an electrolyte containing iodide and tri-iodide. A layer of additional electrolyte separates the porous TiO_2 from a counter electrode. When a photon is absorbed by a dye, the excited dye transfers an electron to the TiO_2 (termed injection). The then oxidized dye can be reduced by iodide (regeneration) or can recapture an electron from the TiO_2. The electron in the TiO_2 can diffuse to a collection electrode (transport) or can be captured by a triiodide molecule in the electrolyte. Electrons that reach the collection electrode flow through the external circuit and reduce tri-iodide to iodide at the counter electrode.

Compared with the conventional single-crystal silicon-based or compound-semiconductor thin-film solar cells, DSSCs are thought to be advantageous as a photovoltaic device possessing both practicable high efficiency and cost effectiveness. To date, the most successful DSSC was obtained on TiO_2 nanocrystalline film combined with a ruthenium–polypyridine complex dye (Gra¨tzel et al., 2000, 2001, 2003 & 2007). Following this idea, a certified overall conversion efficiency of 10.4% was achieved on a TiO_2–RuL′(NCS)3 (''black dye'') system, in which the spectral response of the complex dye was extended into the near-infrared region so as to absorb far more of the incident light. The porous nature of nanocrystalline TiO_2 films drives their use in DSSCs due to the large surface area available for dye-molecule adsorption. Meanwhile, the suitable relative energy levels at the semiconductor–sensitizer interface (i.e., the position of the conduction-band edge of TiO2 being lower than the excited-state energy level of the dye) allow for the effective injection of electrons from the dye molecules to the semiconductor (Nelson & Chandler, 2004).

2. The dye-sensitized solar cell

A promising alternative energy source of DSSC will be expected to increase the significant contribution to overall energy production over the coming years. This is mainly due to the offering a low-cost fabrication and attractive features such as transparency, flexibility, etc.

that might facilitate the market entry. Among all of them, DSSCs are devices that have shown to reach moderate efficiencies, thus being feasible competitors to conventional cells. DSSC combine the optical absorption and charge-separation processes by the association of a sensitizer as light-absorbing material with a wide band-gap semiconductor (usually titanium dioxide). A schematic representation of energy flow in DSSC is illustrated in Figure 1. As early as the 1970s, it was found that TiO_2 from photoelectrochemical cells could split water with a small bias voltage when exposed to light (Fujishima & Honda, 1972). However, due to the large band-gap for TiO_2, which makes it transparent for visible light, the conversion efficiency was low when using the sun as illumination source. This pioneering research involved an absorption range extension of the system into the visible region, as well as the verification of the operating mechanism by injection of electrons from photoexcited dye molecules into the conduction band of the n-type semiconductor. Since only a monolayer of adsorbed dye molecules was photoactive, light absorption was low and limited when flat surfaces of the semiconductor electrode were employed. This inconvenience was solved by introducing polycrystalline TiO_2 (anatase) films with a surface roughness factor of several hundreds Desilvestro et al., 1985). The amount of adsorbed dye was increased even further by using mesoporous electrodes, providing a huge active surface area thereby, and cells combining such electrodes and a redox electrolyte based on iodide/triiodide couple yielded 7% conversion efficiencies in 1991 (Nazeerudin et al., 1993). The next highest energy conversion efficiency is over 11% (Chiba et al., 2006), and further increase of the efficiency is possible by designing proper electrodes and sensitization dyes. Michael Grätzel is a professor at the École Polytechnique Fédérale de Lausanne where he directs the Laboratory of Photonics and Interfaces. He pioneered research on energy and electron transfer reactions in mesoscopic-materials and their optoelectronic applications and discovered a new type of solar cell based on dye sensitized mesoscopic oxide particles and pioneered the use of nanomaterials in lithium ion batteries. Today, record efficiencies above 13% have been presented at an illumination intensity of 1000 Wm-2, and the device displays promising stability data (Gra¨tzel et al., 2000, 2001, 2003 & 2007).

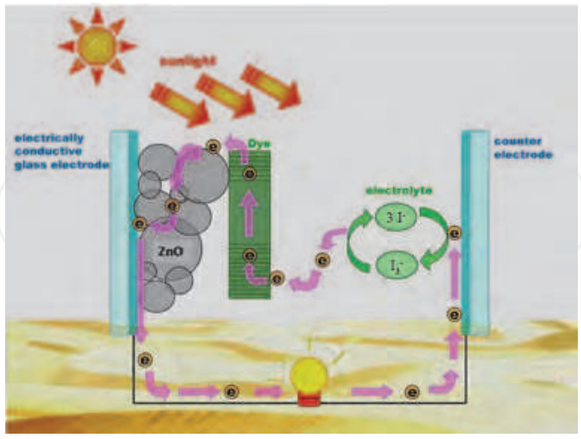

Fig. 1. Schematic diagram of the energy flow in the dye-sensitized solar cell.

The possible mechanism of electron hole interaction during DSSC operation is illustrated in Figure 2. After the successful excitation of dye molecules with the sun light, the ground state electrons at the highest occupied molecular orbital will be photoexcited and residing at unoccupied molecular orbital. Then, the photoexcited electrons are passing through the

nanomaterials to reach electrodes for completion. The detailed mechanism for the electron transports within DSSC device is described as shown in Figure 2. Here, photoexcited electrons are injected from the dye to the conduction band (denoted as ''c.b.'') of the nanocrystallite (1), the dye is regeneratedby electron transfer from a redox couple in the electrolyte (3), and a recombination may take place between the injected electrons and the dye cation (2) or redox couple (4). The latter (4) is normally believed to be the predominant loss mechanism. Electron trapping in the nanocrystallites (5) is also a mechanism that causes energy loss.

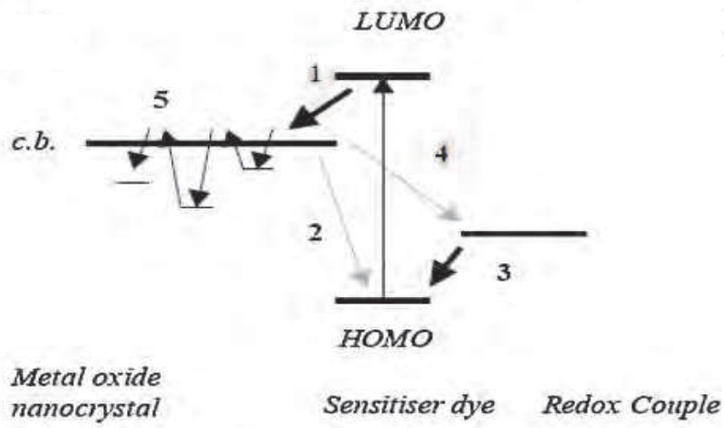

Fig. 2. A schematic illustrates the electron-hole interactions after the excitation of dye molecules with the sun light.

In the recent years, the DSSCs offer to achieve moderate conversion efficiency to the maximum of ~14%. In this case, a wide band gap, mesoporous nanocrystalline TiO_2 was used as photoanodic material, on which dye molecules are adsorbed for the photo harvesting. Major achievers in the DSSC developments are mainly from the recent technology development and optimization. Now in the place of TiO_2, an another alternative, a direct wide band gap metal oxide material is zinc oxide (ZnO), a wurtzite type semiconductor with an energy gap of 3.37 eV at room temperature, as summerziaed in Table 1. Due to its large bandgap, ZnO is an excellent semiconductor material like other wide bandgap materials of GaN and SiC. The crystal strcture, energy band gap, electron mobility and electron diffusion coefficient of both ZnO and TiO_2 nanomaterials were summerized in Table 1, for comparison. The band gap energy of ZnO nanomaterials is almost same as that of TiO_2 and the electron mobility and electron diffusion coefficient of ZnO showed much highier values than the TiO_2, which facilites the important for the DSSC application.

To understand this issue, DSSC technology based on ZnO has been explored extensively. ZnO is a wide-band-gap semiconductor that possesses an energy-band structure and physical properties similar to those of TiO_2 (Table 1), but has higher electronic mobility that would be favorable for electron transport, with reduced recombination loss when used in DSSCs. Hence, many studies have already been started and reported on the useage of ZnO nanomaterial for application in DSSCs. Although the conversion efficiencies of 0.4–5.8% obtained for ZnO are much lower than that of 11% for TiO_2, ZnO is still thought of as a distinguished alternative to TiO_2 due to its ease of crystallization and anisotropic growth. These properties allow ZnO to be produced in a wide variety of nanostructures, thus

presenting unique properties for electronics, optics, or photocatalysis (Tornow et al., 2007 & 2008 and Djurisic et al 2006). Parallely, numerous works have been published to explore in-depth analysis of their shape controllable synthesis that includes needles, rods, tubes, towers, hollow prisms, tetra-legs, flowers, stars, helices, belts and springs via simple method. For example, the major reason for useage of nanostructures with a large specific surface area help in many particular behaviors in electron transport or light propagation in view of the surface effect, quantum-confinement effect or photon localization (Bittkau et al., 2007). Those nanostructural forms of ZnO developed during the past several decades mainly include nanoparticles, nanorod, nanotubes, nanobelts, nanosheets and nanotips. The production of these structures can be achieved through sol–gel synthesis, hydrothermal /solvothermal growth, physical or chemical vapor deposition, low-temperature aqueous growth, chemical bath deposition, or electrochemical deposition.

	ZnO	TiO_2
Crystal structure	rocksalt, zinc blende, and wurtzite	rutile, anatase, and brookite
Energy band gap [eV]	3.2–3.3	3.0–3.2
Electron mobility [$cm^2 Vs^1$]	205–300 (bulk ZnO), 1000 (single nanowire)	0.1–4
Refractive index	2.0	2.5
Electron effective mass[me]	0.26	9
Relative dielectric constant	8.5	170
Electron diffusion coefficient [$cm^2 s^1$]	5.2 (bulk ZnO), 1.7×10^4 (nano-particulate film)	0.5 (bulk TiO_2), 10^8–10^4 (nano- particulate film)

Table 1. A comparison of physical properties of ZnO and TiO_2.

In particular, recent studies on ZnO-nanostructure-based DSSCs have delivered many new concepts, leading to a better understanding of photoelectrochemically based energy conversion. This, in turn, would speed up the development of DSSCs that are associated with TiO_2. Moreover, these ZnO nanomaterials can be synthesized through simple chemical methods with the wide range of structural evolution, fabricating DSSCs with ZnO nano-structured materials will be advisable and reliable in place of TiO_2, whose structural controllability is not easy in a conversional chemical synthetic route. In this chapter, recent developments in ZnO nanostructures, particularly for application in DSSCs, are reported. It will show that photoelectrode films with nanostructured ZnO can significantly enhance solar-cell performance by offering a large surface area for dye adsorption, direct transport pathways for photoexcited electrons, and efficient scattering centers for enhanced light-harvesting efficiency. The limitations of ZnO-based DSSCs are also discussed. In the final section, several attempts to expand ZnO concepts to TiO_2 are presented to motivate further improvement in the conversion efficiency of DSSCs.

3. Crystal and surface structure of ZnO

At ambient pressure and temperature, ZnO crystallizes in the wurtzite (B4 type) structure, as shown in Figure 3 (Jagadish et al., 2006). This is a hexagonal lattice, belonging to the space group $P_{63}mc$ with lattice parameters a = 0.3296 and c = 0.52065 nm. Usually, we can treat it

as a number of two type planes, i.e. tetrahedrally coordinated O^{2-} and Zn^{2+} ions, and stacked alternately along the c-axis. Or in another way, it also can be characterized by two interconnecting sublattices of Zn^{2+} and O^{2-}, such that each Zn ion is surrounded by tetrahedra of O ions, and vice-versa. No doubt, this kind of tetrahedral coordination in ZnO will form a noncentral symmetric structure with polar symmetry along the hexagonal axis, which not only directly induces the characteristic piezoelectricity and spontaneous polarization, but also plays a key factor in crystal growth, etching and defect generation of ZnO.

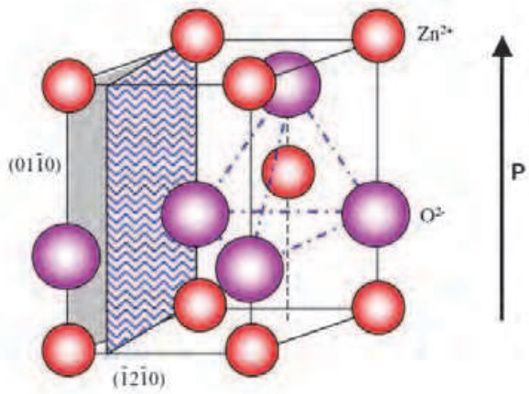

Fig. 3. The wurtzite structure model of ZnO. The tetrahedral coordination of Zn–O is shown.

The polar surface is another important characteristic of ZnO structure. As well as we known, wurtzite ZnO crystallizes do not have a center of inversion. If the ZnO crystals such as nanorods and nanotubes grow along the c axis, two different polar surfaces will be formed on the opposite sides of the crystal due to the suddenly termination of the structure, i.e. the terminated Zn-(0001) surface with Zn cation outermost and the terminated O-(000) surface with O anion outermost. Naturally, these positively charged Zn-(0001) and negatively charged O-(000) surfaces are the most common polar surfaces in ZnO, which subsequently results in a normal dipole-moment and spontaneous polarization along the c-axis as well as a divergence in surface energy. Generally, the polar surfaces have facets or exhibit massive surface reconstructions in order to maintain a stable structure. However, ZnO-± (0001) are exceptions: they are atomically flat, stable and without reconstruction (Dulub et al., 2002 & Wander et al. 2001). Efforts to understand the superior stability of the ZnO ± (0001) polar surfaces are at the forefront of research in today's surface physics (Staemmler et al, 2003 & Singh et al., 2007).

4. Basic physical parameters for ZnO

The basic physical parameters of ZnO were compiled and placed as in Table 2 (Pearton et al., 2005 & Florescu et al., 2002). The physical parameters include energy band gap, excitons binding energy, electron effective mass, hole effective mass, hole hall mobility and lattice paramerter for easy understanding. It should also be noted that there still exists uncertainty in some of these values. For example, there have few reports of p-type ZnO and therefore the hole mobility and effective mass are still in debate. Similarly, the values for thermal conductivity show some spread in values and this may be a result of the influence of defects such as dislocations (Hosokawa et al., 2007), as was the case for GaN. The values for carrier

mobility will undoubtedly increase as more control is gained over compensation and defects in the material.

Physical parameters	Values
Stable phase at 300 K	Wurtzite
Energy band gap	3.37 eV, direct
Density	5.606 g/cm^3
Refractive index	2.008, 2.029
Melting point	1975^{o}C
Thermal conductivity	0.6, 1–1.2
Exciton binding energy	60 meV
Electron effective mass	0.24
Electron Hall mobility at 300 K for low n-type conductivity	200 cm^2/V s
Linear expansion coefficient(/^{o}C)	a_0: 6.5 ×10^{-6} and c_0: 3.0 × 10^{-6}
Static dielectric constant	8.656
Hole effective mass	0.59
Hole Hall mobility at 300 K for low p-type conductivity	5–50 cm^2/V s
Intrinsic carrier concentration	<106 cm^{-3} (max n-type doping >1020 cm^{-3} electrons; max p-type doping <1017 cm^{-3} holes)
Lattice parameters at 300 K	
a_0	0.32495 nm
c_0	0.52069 nm
a_0/c_0	1.602 (ideal hexagonal structure shows 1.633)
U	0.345

Table 2. Physical parameters of ZnO.

5. Synthesis of ZnO nanomaterials for DSSC

The major objective of selecting a photoanodic nanomaterials film for DSSC, it should offer large internal surface area whereby to adsorb sufficient dye molecules for the effect capture of incident photons from the solar power. This objective will be solved by the formation of a porous interconnected network in which the specific surface area may be increased by more than 1000 times when compared with bulk materials (Lee et al., 2003). In this respect, ZnO is a key technological material and it has a wide band-gap compound semiconductor that is suitable for optoelectronic applications. In addition to this, the abundant forms of ZnO nanostructures provide a great deal of opportunities to obtain high surface-area-to-volume ratios, which helps to contribute the successful dye adsorption leading to a better light harvesting, in DSSCs. Therefore, many research groups are actively intriguing to dealings with this task of preparing various structurally different types of ZnO nanostructures to fabricate the DSSC for future energy crisis. Hence, variety of different synthetic methods, such as vapor-phase transport (Zhao et al., 2007, Huang et al., (2001) & Sun et al., (2004), pulsed laser deposition (Wu et al., 2002), chemical vapor deposition (Park et al., 2002, Yu et al., 2005) and electrochemical deposition (Zeng et al., 2006).

Structure	Ru based dyes	Efficiency
Nanoparticles	N719	0.44%, 2.1% (0.06 sun), 2.22%
	N719	5% (0.1 sun)
	N3	0.4%, 0.75%, 2% (0.56 sun), 3.4%
Nanorods	N719	0.73%
	N719	0.22%
	N719	1.69%
Nanotips	N719	0.55%, 0.77%
Nanotubes	N719	1.6%, 2.3%
Nanobelts	N719	2.6%
Nanosheets	N719	2.61%, 3.3%
	N3	1.55%
Nanotetrapods	N719	1.20%, 3.27%
Nanoflowers	N719	1.9%
Nanoporous films	N3	5.08% (0.53 sun)
	N719	3.9%, 4.1%
	N719	0.23%
Nanowires	N3	0.73%, 2.1%, 2.4%, 4.7%
	N719	0.3%, 0.6%, 0.9%,1.5%, 1.54%
Aggregates	N3	3.51%, 4.4%, 5.4%

Table 3. Summary of DSSCs based on ZnO nanostructures.

ZnO nanostructured materials with diverse range of structureally distinct morphologies were synthesized from different methods as listed in Table 3. The detailed behind the morphologically distinct ZnO nanomaterials utilization in the DSSC application with the help of Ru dye complex and their impact of solar power genearation also displayed in Table 3. The followings are the few examples of diverse group of ZnO growth morphologies, such as nanoparticles (Keis et al., 2000, Suliman et al., 2007 & Gonzalez-Valls et al., 2010), nanorod (Lai et al., 2010, Hsu et al., 2008 & Charoensirithavorn et al., 2006), nanotips (Martinson et al., 2007), nanotubes (Lin et al., 2008), nanobelts (Kakiuchi et al., 2008), nanosheets (Chen et al., 2006) , nanotetrapods (Jiang et al, 2007), nanoflowers (Chen et al., 2006), nanoporous films (Hosono et al., 2005, Kakiuchi et al., 2006 & Guo et al., 2005), nanowires (Guo et al., 2005, Rao et al., 2008, Wu et al., 2007 & Law et al., 2005) and aggregates (Chou et al., 2007 & Zhang et al., 2008). These ZnO nanostructures are easily prepared even on cheap substrates such as glass and utilized for the DSSC application as photoanodic materials. Hence, they have a promising potential in the nanotechnology future. The specific impact of individually distinct ZnO nanomaterials will be discussed in the subsequent section in details.

5.1 Useage of ZnO nanoparticles as photoanodic material

The first and foremost interest on ZnO strucutural morphology is of spherical shaped nanoparticles (NPs) that suit in both synthetic methodoly as well as process simplicity. In particular, ZnO NPs can easily be prepared in simple methods by proper judification of their reaction conditions and parameters. Uthirakumar et al. reported simple solution method for the preparation of verity of ZnO nanostructured materials out of which is ZnO NP, one of the significant nanomaterials. The diverse morphology of ZnO nanostructures synthesized from solution method is displayed in Figure 4. They continued to utilize these nanoparticles for

DSSC device fabrication (Uthirakumar et al., 2006, 2007, 2008 & 2009). ZnO NPs with N3 dye sensitizer produced the higher solar power conversion efficiency ranges from 0.44 to 3.4% (Keis et al., 2000, Uthirakumar et al., 2009). However, further improvement of maximum of 5% conversion efficiency with N719 dye. Hosono et al systematically studied the DSSC performance of nanoporous structured ZnO films fabricated by the CBD technique (Hosono et al., 2004, 2005 & 2008). They achieved an overall conversion efficiency of 3.9% when as-prepared 10-mm-thick ZnO films were sensitized by N719 dye with an immersion time of 2 h (Hosono et al., 2005). Further improvement to 4.27% in the conversion efficiency was reported recently by Hosono et al. when the dye of N719 was replaced with a metal-free organic dye named D149 and the immersion time was reduced to 1h (Hosono et al., 2008). The enhancement in solar-cell performance was attributed to the use of D149 dye and a nanoporous structure that contained perpendicular pores. This allowed for a rapid adsorption of the dye with a shorter immersion time and thus prevented the formation of a $Zn^{2}þ$/dye complex. This complex is believed to be inactive and may hinder electron injection from the dye molecules to the semiconductor [66]. In another study, a high photovoltaic efficiency of up to 4.1% was also obtained for nanoporous ZnO films produced by the CBD (Kakiuchi et al., 2006). However, the excellence of the solar-cell performance was ascribed to the remarkably improved stability of as-fabricated ZnO films in acidic dye.

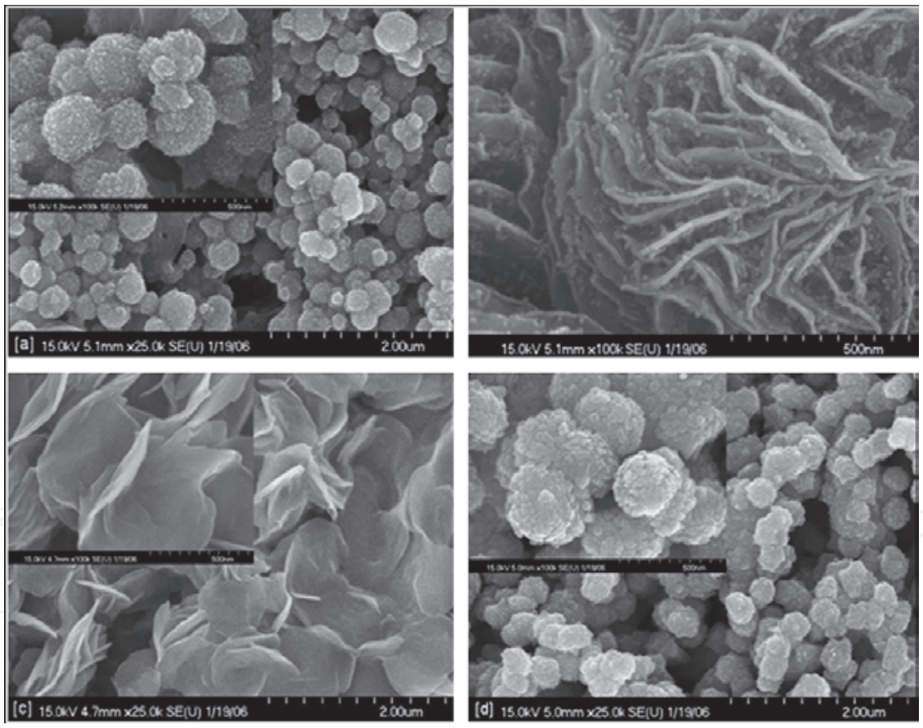

Fig. 4. Diverse morphology of ZnO nanomaterials from solution method.

5.2 Useage of ZnO nanorods as photoanodic material

Controllable length of ZnO nanorods can be grown in solution. The ZnO nanorods are formed at a relatively high temperature (~90 °C), where the reaction solution is enriched with colloidal $Zn(OH)_2$ and therefore allows a fast growth of ZnO nanocrystals along the [001] orientation to form nanorods. ZnO nanorods were grown on the seeded substrates in a

sealed chemical bath containing 10 mM each of zinc nitrate ($Zn[NO_3]_2 \cdot 6H2O$) and hexamine ($[CH2]_6N_4$) for 15 h at 90 ◦C. Photoanodic ZnO nanorod electrodes can be made with vertically-aligned ZnO nanorods and analyzed the usage of DSSC. The highest solar cell efficiency obtained was 0.69% after UV light irradiation (at 72 °C, 0.63 V, 2.85 mA cm^{-2}, 0.39 FF) (Gonzalez-Valls et al., 2010). Typical nanorod-based DSSCs are fabricated by growing nanorods on top of a transparent conducting oxide, as shown in Figure 5. The heterogeneous interface between the nanorod and TCO forms a source for carrier scattering. The new DSSCs yield a power conversion efficiency of 0.73% under 85 mW/cm2 of simulated solar illumination (Lai et al., 2010). Hydrothermally grown and vapor deposited nanorods also exhibit different dependence of photovoltaic performance on the annealing conditions of the rods, indicating significant effect of the native defects on the achievable photocurrent and power conversion efficiency. Efficiency of 0.22% is obtained for both as grown hydrothermally grown nanorods and vapor deposited nanorods annealed in oxygen at 200°C (Hsu et al., 2008). P. Charoensirithavorn et al., proposed a new possibility in designing a cell structure produced an open circuit voltage (Voc) of 0.64 mV, a short circuit current density (Jsc) of 5.37 mA/cm2, a fill factor (FF) of 0.49, and conversion efficiency (η) of 1.69 %, primarily limited by the surface area of the nanorod array (sirithavorn et al., 2006).

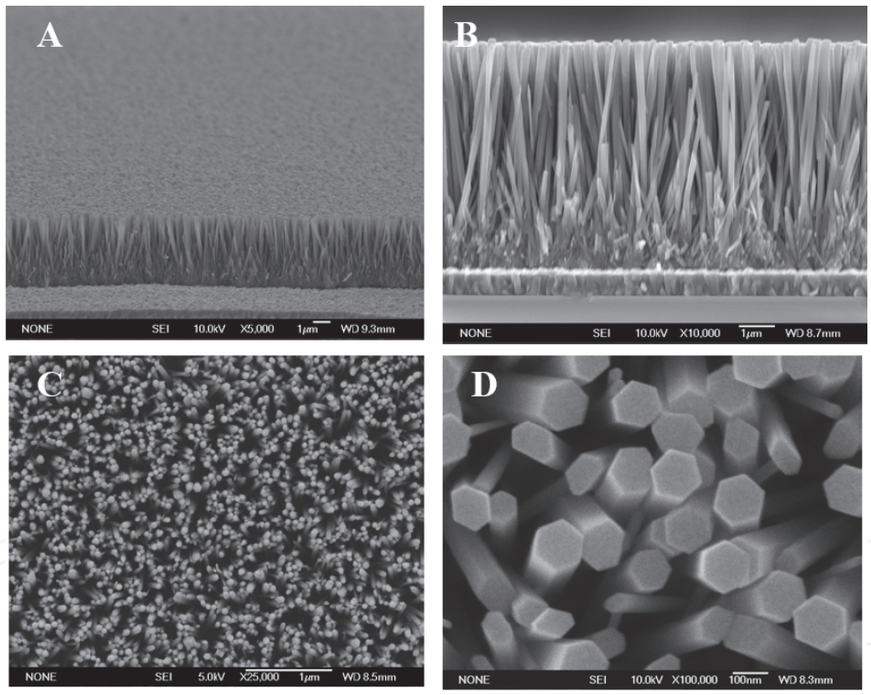

Fig. 4. SEM images of ZnO nanorods grown on FTO substrate (A) tilt, (B) side and (C) top and (D) bottom view at low and high magnification.

5.3 Usage of ZnO nanotubes as photoanodic material

Among one-dimensional ZnO nanostructures, the tubular structures of ZnO become particularly important in DSSC are required their high porosity and large surface area to fulfill the demand for high efficiency and activity. A subsequent decrease in the temperature yields a supersaturated reaction solution, resulting in an increase in the concentration of OH^- ions as well as the pH value of the solution. Colloidal $Zn(OH)_2$ in the supersaturated solution tends to

precipitate continually. However, because of a slow diffusion process in view of the low temperature and low concentration of the colloidal $Zn(OH)_2$, the growth of nanorods is limited but may still occur at the edge of the nanorods due to the attraction of accumulated positive charges to those negative species in the solution, ultimately leading to the formation of ZnO nanotubes, as clearly represented in Figure 5(a). The role of changing the pH value observed in the growth of ZnO crystals is shown also to have a relationship to the change of the surface energy. In the course of growing ZnO nanorods, changing the growth temperature, from a high (90 °C) to a low temperature (60 °C), leads to some change in the pH value. At the low pH value, the polar face has such a high surface energy that it permits the growth of nanorods. However, the grain growth can be inhibited by a high pH value at a low growth temperature. The competition between the change of surface energy due to pH value and growth rate dictated by the temperature can be assumed to lead to the ZnO tube structure, as shown in Figure 5(b). This investigation provides more options and flexibility in controlling methods to obtain various morphologies of ZnO crystals in terms of the change of growth temperature and pH value. Other synthetic methods for the preparation of nanotubes are realized by electrochemical method, low temperature solution method, vapor phase growth and the simple chemical etching process to convert the nanorods into nanotubes. The chemical etching process was carried out by suspending the nanorods sample upside down in 100 ml aqueous solution of potassium chloride (KCl) with 5M concentration for 10 h at 95 °C.

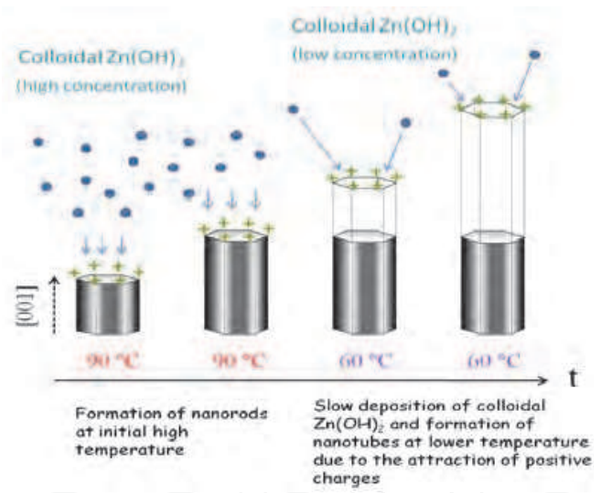

(a)

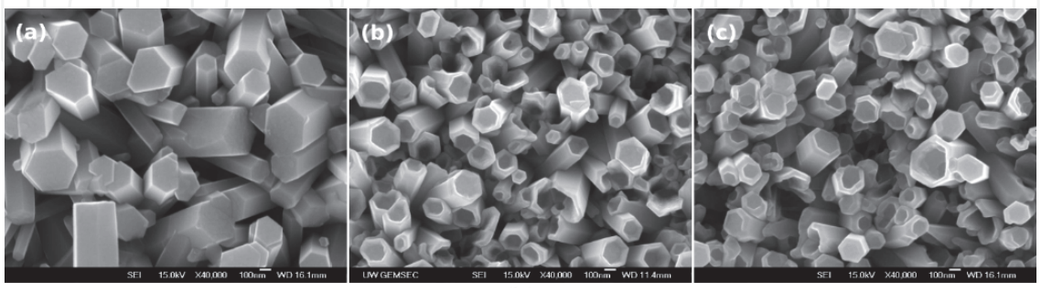

(b)

Fig. 5. A schematic representation and B) SEM images on evolution of ZnO nanorods to tubes while the solution was kept at 90 °C for 3 h and then cooled down to (a) 80 °C (20 h), (b) 60 °C (20 h) and (c) 50 °C (20 h).

High-density vertically aligned ZnO nanotube arrays were fabricated on FTO substrates by a simple and facile chemical etching process from electrodeposited ZnO nanorods. The nanotube formation was rationalized in terms of selective dissolution of the (001) polar face. The morphology of the nanotubes can be readily controlled by electrodeposition parameters for the nanorod precursor. By employing the 5.1 μm-length nanotubes as the photoanode for a DSSC, a full-sun conversion efficiency of 1.18% was achieved (Han *et al.*, 2010). Alex et al introduce high surface area ZnO nanotube photoanodes templated by anodic aluminum oxide for use in dye-sensitized solar cells (DSSCs). Compared to similar ZnO-based devices, ZnO nanotube cells show exceptional photovoltage and fill factors, in addition to power efficiencies up to 1.6%. The novel fabrication technique provides a facile, metal-oxide general route to well-defined DSSC photoanodes (Martinson et al., 2010). Nanotubes differ from nanowires in that they typically have a hollow cavity structure. An array of nanotubes possesses high porosity and may offer a larger surface area than that of nanowires. An overall conversion efficiency of 2.3% has been reported for DSSCs with ZnO nanotube arrays possessing a nanotube diameter of 500 nm and a density of 5.4 $x10^6$ per square centimeter. ZnO nanotube arrays can be also prepared by coating anodic aluminum oxide (AAO) membranes via atomic layer deposition. However, it yields a relatively low conversion efficiency of 1.6%, primarily due to the modest roughness factor of commercial membranes (Chae et al., 2010).

5.4 Usage of ZnO nanowires as photoanodic material

In 2005, Law et al. first reported the usage of ZnO nanowire arrays in DSSCs by with the intention of replacing the traditional nanoparticle film with a consideration of increasing the electron diffusion length (Law et al., 2007). Nanowires were grown by immersing the seeded substrates in aqueous solutions containing 25 mM zinc nitrate hydrate, 25 mM hexamethylenetetramine, and 5–7 mM polyethylenimine (PEI) at 92 8C for 2.5 h. After this period, the substrates were repeatedly introduced to fresh solution baths in order to obtain continued growth until the desired film thickness was reached. The use of PEI, a cationic polyelectrolyte, is particularly important in this fabrication, as it serves to enhance the anisotropic growth of nanowires. As a result, nanowires synthesized by this method possessed aspect ratios in excess of 125 and densities up to 35 billion wires per square centimeter. The longest arrays reached 20–25 mm with a nanowire diameter that varied from 130 to 200 nm. These arrays featured a surface area up to one-fifth as large as a nanoparticle film.

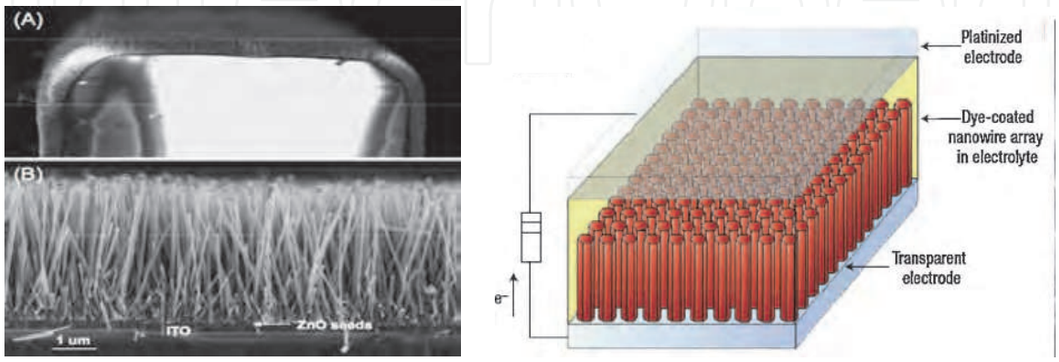

Fig. 6. a) Cross-sectional SEM image of the ZnO-nanowire array and b) Schematic diagram of the ZnO-nanowire dye-sensitized solar cells.

Figure 6a shows a typical SEM cross-section image of an array of ZnO nanowires. It was found that the resistivity values of individual nanowires ranged from 0.3 to 2.0 V cm, with an electron concentration of 1–5 x 10^{18} cm^3 and a mobility of 1–5 cm^2 V^1s^1. Consequently, the electron diffusivity could be calculated as 0.05–0.5 cm^2 s^1 for a single nanowire. This value is several hundred times larger than the highest reported electron diffusion coefficients for nanoparticle films in a DSSC configuration under operating conditions, that is, 10^7–10^4 cm^2 s^1 for TiO_2 and 10^5–10^3 cm^2 s^1 for ZnO. A schematic of the construction of DSSC with nanowire array is shown in Figure 6b. Arrays of ZnO nanowires were synthesized in an aqueous solution using a seeded-growth process. This method employed fluorine-doped tin oxide (FTO) substrates that were thoroughly cleaned by acetone/ethanol sonication. A thin film of ZnO quantum dots (dot diameter ~3–4 nm, film thickness ~10–15 nm) was deposited on the substrates via dip coating in a concentrated ethanol solution. For example, at a full sun intensity of 100 x 3mW cm^2, the highest-surface-area devices with ZnO nanowire arrays were characterized by short-circuit current densities of 5.3–5.85 mA cm^2, open-circuit voltages of 610–710 mV, fill factors of 0.36–0.38, and overall conversion efficiencies of 1.2–1.5% (Kopidakis et al., 2003).

5.5 Usage of ZnO nanoflowers as photoanodic material

Another interesting morphology is of using ZnO nanoflowers as photoanodic materials for DSSC device fabrication. The shape of nanoflower consists of upstanding stem with irregular branches in all sides of base stem and overall it looks like a flower like morphology. Importance of Nanoflower structure is coverage of ZnO-adsorped dye molecules for effective light harvesting than in in nanorod itself. Because of the fact that nanoflower can be stretch to fill intervals between the nanorods and, therefore, provide both a larger surface area and a direct pathway for electron transport along the channels from the branched ''petals'' to the nanowire backbone (Fig. 7). ZnO film consisits of nanoflowers can be grown by a hydrothermal method at low temperatures. The typical procedure is as follows: 5 mM zinc chloride aqueous solution with a small amount of ammonia. These as-synthesized nanoflowers, as shown in Figure 7b, have dimensions of about 200 nm in diameter. Then, the ZnO films with ''nanoflowers'' have been also reported for application in DSSCs. The solar-cell performance of ZnO nanoflower films was characterized by an overall conversion efficiency of 1.9%, a current density of 5.5mA cm^2, and a fill factor of 0.53. These values are higher than the 1.0%, 4.5 mA cm^2, and 0.36 for films of nanorod arrays with comparable diameters and array densities that were also fabricated by the hydrothermal method (Jiang et al., 2007).

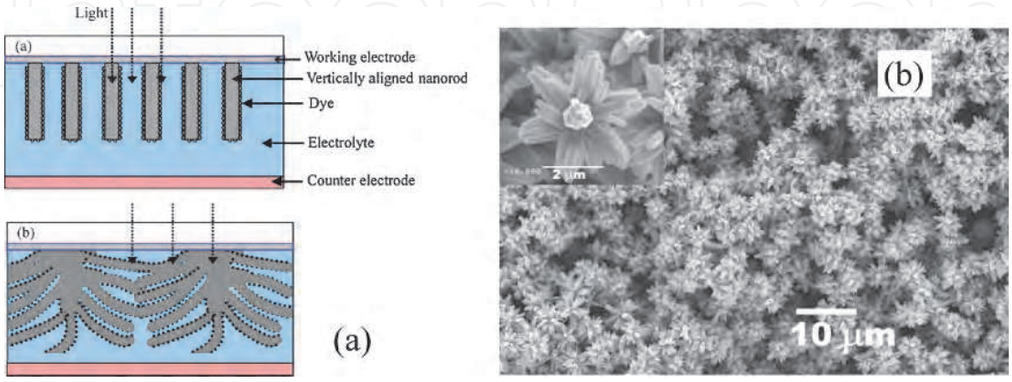

Fig. 7. a) Schematic diagram of the ZnO nanoflower-based dye-sensitized solar cells and b) Top view SEM image of the ZnO-nanoflowers.

5.6 Usage of ZnO nanosheets as photoanodic material

Rehydrothermal growth process of previously hydrothermally grown ZnO nanoparticles can be used to prepare ZnO nanosheets, which are quasi-two-dimensional structures (Suliman et al., 2007, Kakiuchi et al., 2008). Figure 8 shows the SEM images of ZnO nanosheets of low and high magnignified images. ZnO nanosheets are used in a DSSC application, which possess a relatively low conversion efficiency, 1.55%, possibly due to an insufficient internal surface area. It seems that ZnO nanosheetspheres prepared by hydrothermal treatment using oxalic acid as the capping agent may have a significant enhancement in internal surface area, resulting in a conversion efficiency of up to 2.61% (Suliman et al., 2007, Kakiuchi et al., 2008). As for nanosheet-spheres, the performance of the solar cell is also believed to benefit from a high degree of crystallinity and, therefore, low resistance with regards to electron transport.

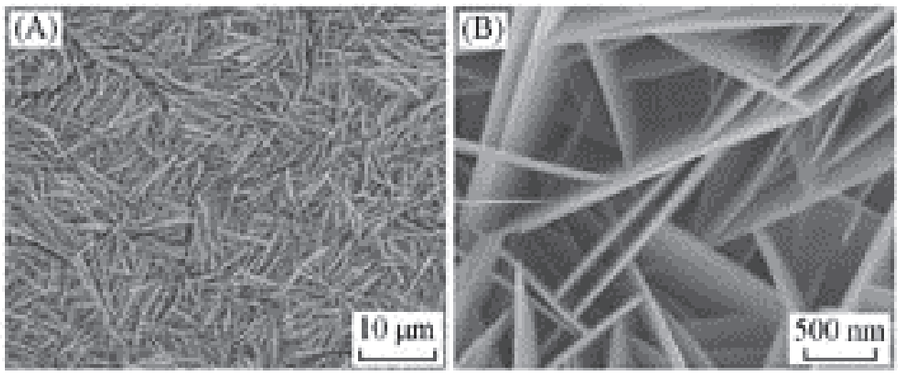

Fig. 8. a) Low and b) High magnified SEM images of the ZnO-nanosheets.

5.7 Usage of ZnO nanobelts as photoanodic material

ZnO nanobelts as photoanodic material can be prepared via an electrodeposition technique. Typically, 1 g of zinc dust mixed with 8 g of NaCl and 4 mL of ethoxylated nonylphenol [$C_9H_{19}C_6H_4(OCH_2CH_2)_nOH$] and polyethylene glycol [$H(OCH_2CH_2)_nOH$], and subsequently ground for one hour. The ground paste-like mixture was loaded into an alumina crucible and covered with a platinum sheet leaving an opening for vapor release. The crucible was then loaded into a box furnace and heated at 800°C. Here, ZnO films consists of nanobelt arrays as shown in Figure 9a and it also proposed to use for DSSC applications. In fabricating these nanobelts, polyoxyethylene cetylether was added in the electrolyte as a surfactant. The ZnO nanobelt array obtained shows a highly porous stripe structure with a nanobelt thickness of 5 nm, a typical surface area of 70 $m^2 g^1$, and a photovoltaic efficiency as high as 2.6%.

5.8 Usage of ZnO nanotetrapods as photoanodic material

A three-dimensional structure of ZnO tetrapod that consisting of four arms extending from a common core, as showin in Figure 9b (Jiang et al., 2007 & Chen et al., 2009). The length of the arms can be adjusted within the range of 1–20 mm, while the diameter can be tuned from 100 nm to 2 mm by changing the substrate temperature and oxygen partial pressure during vapor deposition. Multiple-layer deposition can result in tetrapods connected to each other so as to form a porous network with a large specific surface area. The films with ZnO tetrapods used in DSSCs have achieved overall conversion efficiencies of 1.20– 3.27%. It was

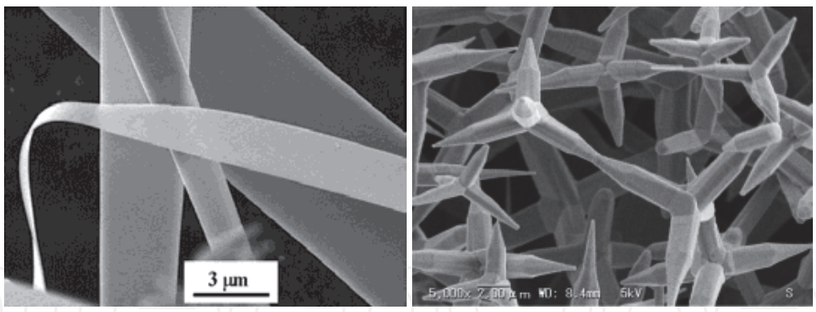

Fig. 9. SEM images of a) ZnO-nanobelt and b) ZnO nanotetrapods.

reported that the internal surface area of tetrapod films could be further increased by incorporating ZnO nanoparticles with these films, leading to significant improvement in the solar-cell performance. Another type of nanomaterials such as nanoporous film also leads to have the maximum coversion efficiency of 4.1% with N719 dye (Hosono et al., 2005).

5.9 Usage of ZnO aggregates as photoanodic material

So far, the maximum overall energy conversion efficiency was reported up to 5.4% from the ZnO film consisits of polydisperse ZnO aggregates, when compared to other nanostructures conversion efficiency of 1.5–2.4% for ZnO nanocrystalline films, 0.5–1.5% for ZnO Nanowire films, and 2.7–3.5% for uniform ZnO aggregate films (Desilvestro et al., 1985, Chou et al., 2007 & Zhang et al., 2008). The overall conversion efficiency of 5.4% with a maximum short-circuit current density of 19mA cm^2 are observed. In other words, the aggregation of ZnO nanocrystallites is favorable for achieving a DSSC with high performance, as shown in Figure 10. This result definitely shock us, since, many gourps were seriously working in synthesizing nanostructured material for DSSC. Here, though the ZnO aggregates are falls in submicron range, individual ZnO nanoparticles are in less than 20 nm. In Figure 10, the film is well packed by ZnO aggregates with a highly disordered stacking, while the spherical aggregates are formed by numerous interconnected nanocrystallites that have sizes ranging from several tens to several hundreds of nanometers. The preparation of these ZnO aggregates can be achieved by hydrolysis of zinc salt in a polyol medium at 160 °C (Chou et al., 2007). By adjusting the heating rate during synthesis and using a stock solution containing ZnO nanoparticles of 5 nm in diameter, ZnO aggregates with either a monodisperse or polydisperse size distribution can be prepared (Zhang et al., 2008).

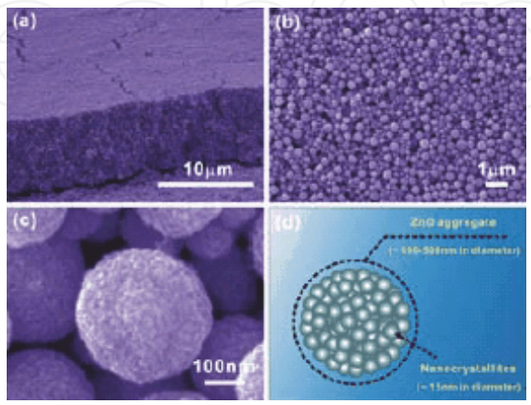

Fig. 10. SEM images of ZnO film with aggregates synthesized at 160 °C and a schematic showing the structure of individual aggregates.

6. Limitation on ZnO-based DSSCs

Although ZnO possesses high electron mobility, low combination rate, good crystallization into an abundance of nanostructures and almost an equal band gap and band position as TiO_2, the photoconversion efficiency of ZnO based DSSC still limited. The major reason for the lower performance in ZnO-based DSSCs may be explained by the a) formation of Zn^{2+}/dye complex in acidic dye and b) the slow electron-injection flow from dye to ZnO. Zn^{2+}/dye complex formation mainly occurs while ZnO is dipped inside the acidic dye solution for the dye adsorption for a long time. Ru based dye molecules consisits of carboxylic functional group for coordination, dye solution mostly existing in acidic medium. Therefore, the Zn^{2+}/dye complex is inevitable. The formation of Zn^{2+}/dye complex has been attributed to the dissolution of surface Zn atoms by the protons released from the dye molecules in an ethanolic solution. For lower electron-injection efficiency is reported of using ZnO material with Ru-based dyes when compared to TiO_2. In ZnO, the electron injection is dominated by slow components, whereas for TiO_2 it is dominated by fast components, leading to a difference of more than 100 times in the injection rate constant. For example, either ZnO or TiO_2, the injection of electrons from Ru-based dyes to a semiconductor shows similar kinetics that include a fast component of less than 100 fs and slower components on a picosecond time scale (Anderson et al., 2003). That is, the ZnO conduction bands are largely derived from the empty s and p orbitals of Zn^{2+}, while the TiO2 conduction band is comprised primarily of empty 3d orbitals from Ti^{4+} (Anderson et al., 2004). The difference in band structure results in a different density of states and, possibly, different electronic coupling strengths with the adsorbate.

7. Alternative dyes for ZnO

According to the limitations of ZnO based DSSC, the lower electron injection and the instability of ZnO in acidic dyes, the alternative type dyes will provide a new pathway for useage of ZnO nanomaterials as photoanodic materials for effective solar power conversion. The list of other alternative dyes were compiled and given in Table 4. The new types of dyes should overcome above mentioned two different limitations and it should be chemically bonded to the ZnO semiconductor for effective for light absorption in a broad wavelength range. Already few research groups were already developed with the aim of fulfilling these criteria. The various new types of dyes include heptamethine-cyanine dyes adsorbed on ZnO for absorption in the red/near-infrared (IR) region (Matsui et al., 2005 & Otsuka et al., 2006 & 2008), and unsymmetrical squaraine dyes with deoxycholic acid, which increases photovoltage and photocurrent by suppressing electron back transport (Hara et al., 2008). Mercurochrome ($C_{20}H_8Br_2HgNa_2O$) is one of the newly developed photosensitizers that, to date, is most suitable for ZnO, offering an IPCE as high as 69% at 510 nm and an overall conversion efficiency of 2.5% (Hara et al., 2008 & Hosono et al., 2004). It was also reported that mercurochrome photosensitizer could provide ZnO DSSCs with a fill factor significantly larger than that obtained with N3 dye, where the latter device was believed to possess a higher degree of interfacial electron recombination due to the higher surface-trap density in the N3-dye-adsorbed ZnO. Eosin Y is also a very efficient dye for ZnO-based DSSCs, with 1.11% conversion efficiency for nanocrystalline films (Rani et al., 2008). When eosin Y is combined with a nanoporous film, overall conversion efficiencies of 2.0–2.4% have been obtained (Hosono et al., 2004 & Lee et al., 2004). Recently, Senevirathne et al. reported that the use of acriflavine (1,6diamino-10-methylacridinium chloride) as a photosensitizer

for ZnO could generate photocurrents that are an order of magnitude higher than in the case of TiO_2 (Senevirathne et al., 2008). Three triphenylamine dyes based on low-cost methylthiophene as the p-conjugated spacer were designed and synthesized as the dye sensitizers for DSSCs applications. The high photovoltaic performances of the DSSCs based on these as-synthesized dyes were obtained. Though the introduction of vinyl unit in the p-conjugated spacer can obtainred-shifted absorption spectra, it does not give a positive effect on the photovoltaic performance of the DSSCs due to unfavorable back-electron transfer and decrease of the open-circuit voltage. On the basis of optimized conditions, the DSSCs based on these three as-synthesized dyes exhibited the efficiencies ranging from 7.83% to 8.27%, which reached 80 to 85% with respect to that of an N719-based device. The high conversion efficiency and easy availability of rawmaterials reveal thatthese metal-free organic dyes are promising in the development of DSSCs (Tian et al., 2010).

Structure	Photosensitizer	Efficiency
Nanoparticles	heptamethine cyanine	0.16%, 0.67
	unsymmetrical squaraine	1.5%
	eosin-Y	1.11%
	acriflavine	0.588%
	mercurochrome	2.5%
Nanoporous films	D149	4.27%
	eosin-Y	2.0%, 2.4%
	eosin-Y	3.31%(0.1 sun)
Nanowires	QDs (CdSe)	0.4%

Table 4. The list of other alternative dyes for ZnO based DSSC.

8. Conclusions

ZnO is believed to be a superior alternative material to replace the existing TiO_2 photoanodic materials used in DSSC and has been intensively explored in the past decade due to its wide band gap and similar energy levels to TiO_2. More important, its much higher carrier mobility is favorable for the collection of photoinduced electrons and thus reduces the recombination of electrons with tri-iodide. Although the formation of Zn^2þ/dye complex is inevitable due to the dissolution of surface Zn atoms by the protons released from the dye molecules in an ethanolic solution, selection of other alternative dye molecules will definitely helps to boost the conversion efficiency to much higher level. Therefore, the recent development on the synthesis of metal-free dye molecules will lead the DSSC device fabrication to the new height as for the cost effectiveness and simple technique are concern.

9. References

Liu, J. (2008). Oriented Nanostructures for Energy Conversion and Storage. Chem. *Sus. Chem.,* 1, pp. 676.

Bagnall, D. M. (2008). *Photovoltaic technologies*. Energ. Pol., 36, pp. 4390.

Chapin D. M. (1954). A new silicon p-n junction photocell for converting solar radiation into electrical power. *J. Appl. Phys.* 25, pp. 676.

Afzaal, M. (2006). Recent developments in II–VI and III–VI semiconductors and their applications in solar cells. *J. Mater. Chem.* 16, pp. 1597.

Birkmire, R. W. (2001). Compound polycrystalline solar cells: Recent progress and Y2 K perspective. *Sol. Energ. Mat. Sol.* 65, pp. 17.

Gratzel, M. (2001). Review article Photoelectrochemical cells. *Nature,* 414, pp. 338.

Gratzel, M. (2000). Perspectives for dye-sensitized nanocrystalline solar cells. *Prog. Photovoltaics*, 8, pp. 171.

Gratzel, M. (2003). Dye-sensitized solar cells. *J. Photochem. Photobiol. C.* 4, pp. 145.

Gratzel, M. (2007). Photovoltaic and photoelectrochemical conversion of solar energy. *Phil. Trans. Math. Phys. Eng. Sci.* 365, pp. 993.

Nelson, J. (2004). Random walk models of charge transfer and transport in dye sensitized systems. *Coord. Chem. Rev*. 248, pp. 1181.

Fujishima, A. (1972). Electrochemical photolysis of water at a semiconductor electrode. *Nature*, 38, pp. 5358.

Desilvestro, J.; Gratzel, M.; Kavan, L.; Moser, J. & Augustynski, J. (1985). Highly Efficient Sensitization of Titanium Dioxide. *Journal of the American Chemical Society,* 107, 10, pp. 2988-2990.

Nazeerudin, M. K. (2003). Conversion of light to electricity by cis-X2bis(2,2'-bipyridyl-4,4'-dicarboxylate)ruthenium(II) charge-transfer sensitizers (X = Cl-, Br-, I-, CN-, and SCN-) on nanocrystalline titanium dioxide electrodes *Journal.of the American Chemical Society* 115, 14, pp. 6382.

Chiba, Y. (2006). Conversion efficiency of 10.8% by a dye-sensitized solar cell using a TiO2 electrode with high haze. *Applied Physics Letters*, 88, 22 pp. 223505.

Tornow, J. Transient Electrical Response of Dye-Sensitized ZnO Nanorod Solar Cells. *J. Phys. Chem. C.* 111, pp. 8692.

Djurisic, A.B. (2006). Optical Properties of ZnO Nanostructures. *Small.* 2, pp. 944.

Tornow, J. (2008). Voltage bias dependency of the space charge capacitance of wet chemically grown ZnO nanorods employed in a dye sensitized photovoltaic cell. *Thin Solid Films.* 516, pp. 7139.

Bittkau, K. (2007). Near-field study of optical modes in randomly textured ZnO thin films. *Superlatt. Microstuct.* 42, pp. 47.

Xi, Y.Y. (2008). Electrochemical Synthesis of ZnO Nanoporous Films at Low Temperature and Their Application in Dye-Sensitized Solar Cells . *J. Electrochem. Soc.* 155, pp. D595.

Jagadish, C. (2006). Zinc oxide bulk, thin films and nanostructures: processing, properties and applications, Publisher: Elsevier Science, 1 edition, pp 3.

Dulub, O. (2002). STM study of the geometric and electronic structure of ZnO(0001)-Zn, (0001)-O, (1010), and (1120) surfaces, *Surf. Sci.* 519, pp. 201-217.

Wander, A. (2001). Stability of polar oxide surfaces, *Phys.Rev. Lett.* 86, pp. 3811-3814.

Staemmler, V. (2003). Stabilization of polar ZnO surfaces: validating microscopic models by using CO as a probe molecule, *Phys. Rev. Lett.* 90, pp. 106102-1-4.

Singh, S. (2007). Structure, microstructure and physical properties of ZnO based materials in various forms: bulk, thin film and nano, *J. Phys. D: Appl. Phys.* 40, pp. 6312-6327.

Pearton, S.J. (2005). Recent progress in processing and properties of ZnO, *Progress in Materials Science*. 50, pp. 293- 340.

Florescu, D. (2002). High spatial resolution thermal conductivity of bulk ZnO (0001), *J Appl Phys.* 91, pp. 890-892.

Hosokawa, M. (2007). Nanoparticle Technology Handbook Elsevier, Amsterdam.

Lee, J. S. (2003). ZnO nanomaterials synthesized from thermal evaporation of ballmilled ZnO powders, *J. Cryst. Growth.* 254, pp. 423-431.

Zhao, Q. X. (2007). Growth of ZnO nanostructures by vapor–liquid–solid method, *Appl. Phys. A*, 88, pp. 27-30.

Huang, M. H. (2001). Catalytic growth of zinc oxide nanowires by vapor transport, *Adv. Mater.* 13, pp. 113- 116.

Sun, Y. (2004). Growth of aligned ZnO nanorod arrays by catalyst-free pulsed laser deposition methods, *Chem. Phys. Lett.* 39, pp. 621-26.

Wu, J . (2002). Low-temperature growth of well-aligned ZnO nanorods by chemical vapor deposition, *Adv .Mater*. 14, pp. 215-218.

Park, W. I. (2002). Metalorganic vapor-phase epitaxial growth of vertically well-aligned ZnO nanorods, *Appl. Phys. Lett.* 80, pp. 4232-4234.

Yu, H. D. (2005). A general lowtemperature route for large-scale fabrication of highly oriented ZnO nanorod/nanotube arrays. *J. Am. Chem. Soc.* 127, pp. 2378-2379.

Zeng, L.Y. (2006). Dye-Sensitized Solar Cells Based on ZnO Films. *Plasma Sci. Tech*. 2006, 8, pp. 172.

Keis, K. (2000). Studies of the Adsorption Process of Ru Complexes in Nanoporous ZnO Electrodes. *Langmuir*. 16, pp. 4688.

Suliman, A.E.(2007). Preparation of ZnO nanoparticles and nanosheets and their application to dye-sensitized solar cells Sol. *Energ. Mat. Sol. Cells*. 91, pp. 1658.

Gonzalez-Valls, I. (2010). Dye sensitized solar cells based on vertically-aligned ZnO nanorods: effect of UV light on power conversion efficiency and lifetime. *Energy Environ. Sci*., 3, pp. 789-795.

Lai, M. H. (2010). ZnO-Nanorod Dye-Sensitized Solar Cells: New Structure without a Transparent Conducting Oxide Layer. *International Journal of Photoenergy,* pp. Article ID 497095, 5 pages

Hsu, Y.F. (2008). ZnO nanorods for solar cells: Hydrothermal growth versus vapor deposition, *Appl. Phys. Lett.* 92, pp. 133507.

Chen, H.H. (2008). Dye-sensitized solar cells using ZnO nanotips and Ga-doped ZnO films. *Semicond. Sci. Technol.* 23, pp. 045004.

Martinson, A.B.F. (2007). ZnO Nanotube Based Dye-Sensitized Solar Cells. *Nano Lett*. 7, pp. 2183.

Lin, C. F. (2008). Electrodeposition preparation of ZnO nanobelt array films and application to dye-sensitized solar cells. J. *Alloys Compd*. 462, pp. 175.

Kakiuchi, K. (2008). Fabrication of ZnO films consisting of densely accumulated mesoporous nanosheets and their dye-sensitized solar cell performance. *Thin Solid Films.* 516, pp. 2026.

Chen, W. (2009). A new photoanode architecture of dye sensitized solar cell based on ZnO nanotetrapods with no need for calcination. *Electrochem. Commun.* 11, pp. 1057.

Jiang, C. Y. (2007). Improved dye-sensitized solar cells with a ZnO-nanoflower photoanode. *Appl. Phy. Lett.* 90, pp. 263501.

Chen, Z.G. (2006). Electrodeposited nanoporous ZnO films exhibiting enhanced performance in dye-sensitized solar cells. *Electrochim. Acta.* 51, pp. 5870.

Hosono, E. (2005). The Fabrication of an Upright-Standing Zinc Oxide Nanosheet for Use in Dye-Sensitized Solar Cells. *Adv. Mater.* 17, pp. 2091.

Kakiuchi, K. (2006). Enhanced photoelectrochemical performance of ZnO electrodes sensitized with N-719. *J. Photochem. Photobiol. A* 179, pp. 81.

Guo, M. (2005). Hydrothermal growth of perpendicularly oriented ZnO nanorod array film and its photoelectrochemical properties. *Appl. Surf. Sci.* 249, pp. 71.

Guo, M. (2005). The effect of hydrothermal growth temperature on preparation and photoelectrochemical performance of ZnO nanorod array films. J. Solid State Chem. 178, pp. 3210.

Rao, A. R. (2008). Achievement of 4.7% conversion efficiency in ZnO dye-sensitized solar cells fabricated by spray deposition using hydrothermally synthesized nanoparticles. *Nanotechnology*. 19, pp. 445712.

Wu, J. J. (2007). Effect of dye adsorption on the electron transport properties in ZnO-nanowire dye-senstized solar cells. *Appl. Phy. Lett*. 2007, 90, pp. 213109.

Law, M. (2005). Nanowire dye-sensitized solar cells. *Nat. Mater.* 4, pp. 455.

Zhang, R. (2008). High-Density Vertically Aligned ZnO Rods with a Multistage Terrace Structure and Their Improved Solar Cell Efficiency. *Cryst. Growth Des.* 8, pp. 381.

Chou, T.P. (2007). Hierarchically Structured ZnO Film for Dye-Sensitized Solar Cells with Enhanced Energy Conversion Efficienc. *Adv. Mater.* 19, pp. 2588.

Zhang, Q.F. (2008). Polydisperse aggregates of ZnO nanocrystallites: a method for energy-conversion-efficiency enhancement in dye-sensitized solar cells, *Adv. Funct. Mater*. 18, pp. 1654.

Chou, T.P. (2007). Effects of Dye Loading Conditions on the Energy Conversion Efficiency of ZnO and TiO_2 Dye-Sensitized Solar Cells. *Phys. Chem. C.* 111, pp.18804.

Uthirakumar, p. (2006). ZnO nanoballs synthesized from a single molecular precursor via non-hydrolytic solution route without assistance of base, surfactant, and template etc . *Phys. Lett. A,* 359, pp. 223.

Uthirakumar, p. (2007). Nanocrystalline ZnO particles: Low-temperature solution approach from a single molecular precursor. *J. Cryst. Growth*. 304, pp. 150.

Uthirakumar, p. (2009). Zinc Oxide Nanostructures Derived from a Simple Solution Method for Solar Cells and LEDs. *Chemical Engineering Journal*, 155, pp. 910-915.

Uthirakumar, p. (2009). Effect of Annealing Temperature and pH on the Morphology and Optical Properties of Highly Dispersible ZnO nanoparticles. *Material Characterization*, 60(11), pp. 1305-1310.

Eom, S. H. (2008). Preparation and characterization of nano-scale ZnO as a buffer layer for inkjet printing of silver cathode in polymer solar cells. *Sol. Energy Mater. Sol. Cells,* 92, pp. 564.

Hosono, E. (2004). Growth of layered basic zinc acetate in methanolic solutions and its pyrolytic transformation into porous zinc oxide films. *J. Colloid Interface Sci.* 272, 391.

Hosono, E. (2008). Metal-free organic dye sensitized solar cell based on perpendicular zinc oxide nanosheet thick films with high conversion efficiency. *Dalton Trans.* pp. 5439.

Charoensirithavorn, P. (2006). Dye-sensitized Solar Cell Based on ZnO Nanorod Arrays. *The 2nd Joint International Conference on Sustainable Energy and Environment.* 21-23 November 2006, Bangkok, Thailand.

Han, J. (2010). ZnO nanotube-based dye-sensitized solar cell and its application in self-powered devices, *Nanotechnology* 21, pp. 405203.

Martinson, A.B.F. (2007). ZnO Nanotube Based Dye- ensitized Solar Cells. *Nano letters*. 7, pp. 2183.

Chae, K. W. (2010). Low-temperature solution growth of ZnO nanotube arrays, *Beilstein J. Nanotechnol.* 1,pp. 128–134.

Kopidakis, N. (2003). Transport-Limited Recombination of Photocarriers in Dye-Sensitized Nanocrystalline TiO_2 Solar Cells. *J. Phys. Chem. B*. 107, pp. 11307.

Zhang, Q. (2010). Synthesis of ZnO Aggregates and Their Application in Dye-sensitized Solar Cells. *Material Matters*. *5.2,* pp. 32.

Anderson, N.A. (2003). X. Ai,T.Q. Lian, Electron Injection Dynamics from Ru Polypyridyl Complexes to ZnO Nanocrystalline Thin Films. *J. Phys. Chem. B* 107, pp. 14414.

Anderson, N.A. (2004). Ultrafast electron injection from metal polypyridyl complexes to metal-oxide nanocrystalline thin films. *Coord. Chem. Rev.* 248, pp. 1231.

Matsui, M. (2005). Application of near-infrared absorbing heptamethine cyanine dyes as sensitizers for zinc oxide solar cell . *Synth. Met.* 148, pp. 147.

Otsuka, A. (2008). Simple Oligothiophene-Based Dyes for Dye-Sensitized Solar Cells (DSSCs): Anchoring Group Effects on Molecular Properties and Solar Cell Performance. *Chem. Lett.* 37, pp. 176.

Otsuka, A. (2006). Dye Sensitization of ZnO by Unsymmetrical Squaraine Dyes Suppressing Aggregation. *Chem. Lett.* 35, pp. 666.

Hara, K. (2003). Molecular Design of Coumarin Dyes for Efficient Dye-Sensitized Solar Cells. *Phys. Chem. B*, 107 (2), pp 597–606.

Hara, K. (2000). Highly efficient photon-to-electron conversion with mercurochrome-sensitized nanoporous oxide semiconductor solar cells. *Sol. Energ. Mat. Sol. Cells.* 64, pp. 115.

Hosono, (2004). Synthesis, structure and photoelectrochemical performance of micro/nano-textured ZnO/eosin Y electrodes. *Electrochim. Acta.* 49 (14), pp. 2287.

Rani, S. (2008). Synthesis of nanocrystalline ZnO powder via sol–gel route for dye-sensitized solar cells. *Sol. Energ. Mat. Sol. Cells.* 92, pp. 1639.

Lee, W. J. (2004). Fabrication and Characterization of Eosin-Y-Sensitized ZnO Solar Cell, *Jpn. J. Appl. Phys.* 43, pp. 152.

Senevirathne, M.K.I. (2008). Sensitization of TiO_2 and ZnO nanocrystalline films with acriflavine. *Photochem. Photobiol. A*. 195, pp. 364.

Tian, Z. (2010). Low- cost dyes based on methylthiophene for high-performance dye-sensitized solarcells. *Dyes and Pigments* 87, pp. 181-187.

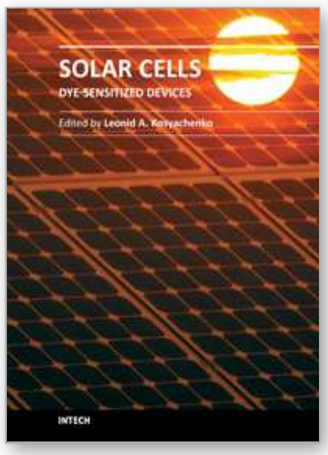

Solar Cells - Dye-Sensitized Devices
Edited by Prof. Leonid A. Kosyachenko

ISBN 978-953-307-735-2
Hard cover, 492 pages
Publisher InTech
Published online 09, November, 2011
Published in print edition November, 2011

The second book of the four-volume edition of "Solar cells" is devoted to dye-sensitized solar cells (DSSCs), which are considered to be extremely promising because they are made of low-cost materials with simple inexpensive manufacturing procedures and can be engineered into flexible sheets. DSSCs are emerged as a truly new class of energy conversion devices, which are representatives of the third generation solar technology. Mechanism of conversion of solar energy into electricity in these devices is quite peculiar. The achieved energy conversion efficiency in DSSCs is low, however, it has improved quickly in the last years. It is believed that DSSCs are still at the start of their development stage and will take a worthy place in the large-scale production for the future.

InTech Europe
University Campus STeP Ri
Slavka Krautzeka 83/A
51000 Rijeka, Croatia
Phone: +385 (51) 770 447
Fax: +385 (51) 686 166
www.intechopen.com

InTech China
Unit 405, Office Block, Hotel Equatorial Shanghai
No.65, Yan An Road (West), Shanghai, 200040, China
中国上海市延安西路65号上海国际贵都大饭店办公楼405单元
Phone: +86-21-62489820
Fax: +86-21-62489821

IntechOpen